# EXPERIMENTAL AND NUMERICAL VALIDATION OF AN ANALYTICAL CALCULATION METHOD FOR NOTCHED FIBRE-REINFORCED MULTILAYERED COMPOSITES UNDER BENDING AND COMPRESSIVE LOADS

B. Grüber*, W. Hufenbach, R. Gottwald, M. Lepper, B. Zhou
Institute of Lightweight Engineering and Polymer Technology (ILK),
Technische Universität Dresden, Holbeinstraße 3, 01307 Dresden, Germany
* Corresponding author (bernd.grueber@tu-dresden.de)

**Keywords**: *Stress concentrations, Analytical functions, Finite outer boundary, Textile composites*

## 1 Introduction

Structures made from fibre- or textile-reinforced composites are gaining in importance over the past years. To utilize the large lightweight potential of this group of materials, it is indispensable to provide adapted calculation concepts and tools for the analysis of critical areas such as the stress concentrations in the vicinity of cut-outs. Since holes in composites can often be considered as design drivers for the whole construction, an analytical method for the stress concentration analysis for multilayered anisotropic plates has been developed [1, 2] which can help the design engineer to take such critical areas into consideration already in an early state of the design process.

For the verification of this method and its implementation, besides the comparison with numerical results, a number of experimental investigations have been carried out, using adapted measurement methods for large deflections and a newly developed test rig for in-plane compression loading.

## 2 Analytical calculation methods

The latest development of the analytical calculation method (see also [1, 2]) takes into account both a finite outer boundary – which is necessary to apply non-constant outer loadings – and the effects of extension-bending-coupling – which may occur when using unsymmetrical composites. The calculation model is based on the assumptions of linear elasticity, small deformation gradients and a plane stress state so that the classical laminate theory (CLT) can be applied. In this case the behavior of the composite is described by the well known structural law of the CLT:

$$\begin{bmatrix} N_x \\ N_y \\ N_{xy} \\ M_x \\ M_y \\ M_{xy} \end{bmatrix} = \begin{bmatrix} A_{11} & A_{12} & A_{16} & B_{11} & B_{12} & B_{16} \\ A_{12} & A_{22} & A_{26} & B_{12} & B_{22} & B_{26} \\ A_{16} & A_{26} & A_{66} & B_{16} & B_{26} & B_{66} \\ B_{11} & B_{12} & B_{16} & D_{11} & D_{12} & D_{16} \\ B_{12} & B_{22} & B_{26} & D_{12} & D_{22} & D_{26} \\ B_{16} & B_{26} & B_{66} & D_{16} & D_{26} & D_{66} \end{bmatrix} \cdot \begin{bmatrix} \varepsilon_x^0 \\ \varepsilon_y^0 \\ \gamma_{xy}^0 \\ \kappa_x \\ \kappa_y \\ \kappa_{xy} \end{bmatrix} \quad (1)$$

with

| | |
|---|---|
| $N_i$, $M_i$ : | force and moment resultants, |
| $A_{ij}$, $B_{ij}$, $D_{ij}$ : (i,j = 1, 2, 6) | extensional, extension-bending-coupling, bending stiffness, |
| $\varepsilon_i^0$ , $\gamma_j^0$ , $\kappa_k$ : | distortions and curvatures of neutral plane. |

Starting with these fundamental assumptions, the method of complex-valued potential functions in combination with conformal mappings and the method of boundary collocation on the finite outer boundary are used to express the stress, displacement and strain fields in the whole finite plate with circular or elliptical cut-out by four analytical functions. The following ansatz is chosen for the solution of the derived system of three coupled partial differential equations which is transformed into one differential equation of order eight in $w_0$:

$$w_0 = 2\,\mathrm{Re}\left( \sum_{k=1}^{4} \Psi_k(\zeta_k) \right), \quad (2)$$

what leads to

$$u_0 = 2\,\mathrm{Re}\left(\sum_{k=1}^{4} p_k \varphi_k(\zeta_k)\right),\ v_0 = 2\,\mathrm{Re}\left(\sum_{k=1}^{4} q_k \varphi_k(\zeta_k)\right) \qquad (3)$$

with

$$\varphi_k(\zeta_k) = (1+\lambda_k)\frac{d\Psi_k(\zeta_k)}{d\zeta_k} \quad (k = 1,\ldots,4) \qquad (4)$$

and eight complex parameters $p_k$, $q_k \in \mathbb{C}$.

For the consideration of the boundary conditions and the loads on the inner and outer plate boundary, the actual stress state is decomposed using the superposition principle (Fig. 1) in the following way:

I: a finite, unnotched plate loaded on the outer edge
II: a finite notched plate loaded at the edge of the notch, whereby with superposition of I and II an overall unloaded notch edge results,
III: a finite notched plate with a loaded notch edge according to the given original boundary conditions.

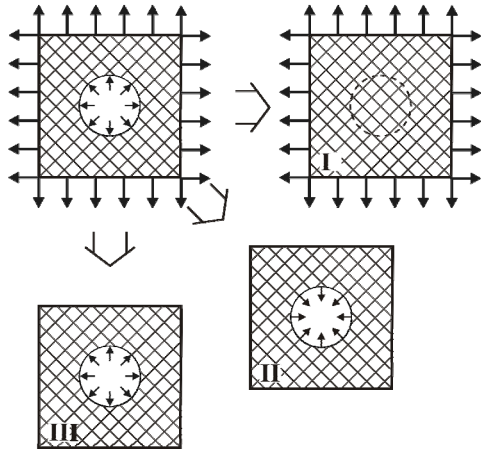

Fig. 1. Decomposition of the coupled membrane-bending problem by principle of superposition

Finally, the coefficients of the principal and the regular part of the LAURENT series representations of the analytical functions are determined by development of the boundary conditions into LAURENT series on the inner boundary, a comparison of coefficients on the inner boundary, analytical continuation of the potential functions onto the whole area of the notched plate and using a combination of boundary collocation method and least squares method for fulfilling the boundary conditions on the outer boundary (see also [3-5] for more in-depth information about the historical and theoretical background).

The developed calculation method allows – within the limitations of the CLT – a layer-by-layer analysis of the whole stress-strain-displacement field in a notched multi-layered composite (MLC).
It has been implemented in an easy-to-use software tool and is to be further verified by extensive experimental and numerical investigations in the ongoing research.
While the analytically based calculation tool offers high potential for an in-depth theoretical insight into the complex behavior of composites in the vicinity of cut-outs, the long-term is as well to use the method in the sense of an analytical sub model e.g. in combination with a Finite Element Analysis (FEA) System.

**3 Experimental and numerical validation**

In extensive parameter studies the developed analytically based calculation tool is validated by comparison with numerically and experimentally gained results. Therefore, investigations were carried out on composite specimens made of multilayer weft knitted fabrics with thermoplastic polymer matrix within the subproject B2 of the collaborative research centre SFB 639. From [5, 6] as well as from preliminary tests, it is known that geometrical ratios concerning length or width depending on e. g. the notch size have to be met when dimensioning the specimen. The geometric and material properties of the standard specimens chosen for the validation are shown in Table 1.

The numerical simulations are carried out using the finite element (FE) system ANSYS 14.0. The four-node element type SHELL181 is applied for the plate models with cut-out in the present study.

For the experimental strain analysis presented here, the optical measurement system ARAMIS (GOM mbH, Braunschweig, Germany) is used. This 3D image correlation technique provides the non-contact measurement of specimens with arbitrary geometries and materials. The strain measuring ac-

curacy of the applied ARAMIS 5M system configuration is 0.01 %. Further information to the background of the measurement system can be found in [7].

Tab. 1. Data of the investigated specimen

| | |
|---|---|
| **Geometry of specimens** | |
| Length | 800 mm |
| Width | 150, 120, 80, 60 mm |
| Thickness | 2.16 mm |
| Diameter of central cut-out | 30 mm |
| **Composite set-up** | |
| Material | Multilayer weft knitted fabrics (MLG) V1a |
| Stacking sequence | $[0/90]_s$ |
| **Material properties of single bi-directionally knitted fabrics made of reinforced lamina from hybrid glass-fibre-polypropylene yarn** | |
| $E_1$ | 21.5 GPa |
| $E_2$ | 20.7 GPa |
| $G_{12}$ | 1.86 GPa |
| $\nu_{12}$ | 0.13 |

For the validation the gained results of the decay behavior of the analytical, numerical and experimental strains were determined and compared at radial sections in x-, (0°-) and y-, (90°-) direction at the maximum chosen testing force and the maximum given displacement respectively.

### 3.1 Findings from former investigations

**Former tensile tests**
In [1, 2] first analytical, numerical and experimental validation studies concerning notched specimens under tensile load were already presented, the achieved results will be summarized here only shortly.

In the numerical studies the following examinations on the influence of the specimen geometry, the boundary conditions and loads on the results were carried out.

- Variation of specimen width and length
- Variation of plate orientation with respect to the cut-out (chosen case: elliptic cut-out)
- Use of locally varying boundary loads

To sum up the result, a good correlation of the analytically and numerically calculated results was observed. Within the investigations, an improvement of the settings of the analytical model concerning the used boundary collocation method was also achieved.

**Preliminary studies to compression and flexure tests**
In preliminary experimental and numerical investigations, it turned out that especially if dealing with locally high strain gradients, as they occur in the case of loaded composites with cut-outs, the available testing devices e.g. for flexure or in-plane compression have large deficits. The here investigated thin walled notched specimens made of fibre-reinforced multilayered composites need to have a certain length to avoid undesired influences on the results caused by the chosen method of load introduction [5]. For that reason, these specimens used in conventional experimental set-ups, cannot be loaded by a pure flexural moment in standard flexure testing devices and they tend to buckle already at very low compressive loads in standard compression testing devices respectively.
However, no suited test devices were found by the authors, to analyze specimens with practically relevant dimensions. To overcome this shortcoming, new testing and measurement technologies had to be developed.

### 3.2 Validation at in-plane compression

The known devices for the examination of thin-walled specimens under in-plane compression loading (e. g. [6, 8, 9]) are not suited for the aim of analyzing the strain behavior of structures with cut-outs. The suggested gauge length dimensions are often too short for the investigation of structures with given notch diameters. The principles of the testing devices which allow the examination of larger specimens are based on specimen support. However, it is assumed that these offer too much friction loss, caused by sliding friction of the friction combination steel/plastic intensified by a resulting transverse strain.

**Investigations for a novel in-plane compression testing device**
A better solution for the in-plane compression test of plane thin walled composites with large length and width dimensions including the possibility to define an adjustable measuring field is introduced in [10]. Here the construction and functionality of a

novel testing device is described. Several investigations as well as the applicability for the experimental stress-strain concentration analysis of multilayer textile composites under in-plane compressive load are presented exemplarily.

The main aspects of the novel testing device will be explained here only shortly, for more in-depth information see [10].
Starting on the assumption that the standard specimen with its large length of 800 mm (see also Table 1) would tend to buckle under in-plane compressive load, the aim is to shorten the free length of the specimen by supporting the plate locally and therewith to increase the critical compressive force.
In numerical investigations on the plate structure with cut-out, the buckling behavior is studied. Initially the unsupported specimen is simulated having boundary conditions comparable to the EULER buckling case 2 at a free specimen length of 800 mm. It shows a stability failure at an in-plane compression load of $F_x$=40.5 N (see Fig. 2).


Fig. 2. First buckling mode of the unsupported standard specimen at a critical compressive force of $F_x$=40.5 N

Further simulations confirm that the critical compressive force can be raised systematically by supporting the specimen with locally arranged supporting elements. Therefore low-friction support elements, e.g. analogous to ball bearings, were chosen and introduced by a contact formulation in the analysis.

To ensure well measurable strain fields for the experimental investigations, a load of about $F_x$=4.0 kN in axial direction is chosen as rough target. This maximum compressive force to be applied is comparable to that used in former tensile tests and is supposed to cause no inelastic material behavior in the specimen. The load application at the current development status is realized by inducing the compressive force to the specimen with mounted load application adapters simulated here by coupling the nodes of the plate model at that according region (that means a resulting free specimen length of 700 mm). More details to the model and the defined arrangement of the supporting bearings respectively are provided in Fig. 3 and Table 2.

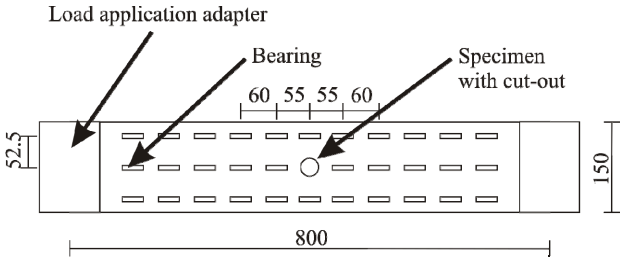


Fig. 3. Arrangement of supporting bearings and load application adapters for in-plane compression loading of thin-walled specimen with cut-out [10]

Tab. 2. Selected data of the simulation model, setup in ANSYS 14.0

| | |
|---|---|
| **Summary to finite element model** | |
| Number of elements | 38972 |
| Number of nodes | 25002 |
| **Element types** | |
| Plate element type | SHELL181 |
| Plate contact type | CONTA173 |
| Bearing contact type | TARGE170 |
| **Geometrical data of supporting bearings** | |
| Bearing diameter | 35 mm |
| Contacting bearing width | 6.5 mm |
| **Adjustment of supporting bearings** | |
| x-distance of bearings | 60 mm |
| x-distance of bearings at measurement region | 55 mm |
| y-distance of bearings | 52.5 mm |

The first characteristic buckling mode is simulated and a critical compressive force of $F_x$=4.5 kN is identified (displayed in Fig. 4). The instability occurs outside the measurement region at the load

introduction area, which is seen as an advantage for avoiding undesired influence of the testing device to the measurement.

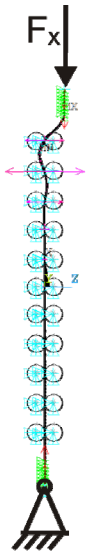


Fig. 4. First buckling mode of the supported standard specimen at a critical compressive force of $F_x$=4.5 kN

**Numerical determination of the strain decay behaviour**

For the numerical validation of the analytical calculation method the simulation model of the notched plate structure taken for the development of the novel type of compression testing device is used.

Therefore, analogous to the experimental investigations in the following, the influence of varying specimen width on the strain results under in-plane compressive load is numerically simulated. The composite plates with cut-outs are loaded with axial compressive forces $F_x$ as displayed in Table 3 so that for all specimens the stress in the undisturbed region is equal to $\sigma_x$=11.575 MPa.

Tab. 3. Specimen and load parameters for stress concentration analysis under in-plane compressive load

| Specimen width [mm] | 60 | 80 | 120 | 150 |
|---|---|---|---|---|
| Compressive force [kN] | 1.5 | 2.0 | 3.0 | 3.75 |
| Ratio force/unnotched width [N/mm] | 25 | 25 | 25 | 25 |
| Ratio force/notched width [N/mm] | 50 | 40 | 33.3 | 31.25 |

The strain decay behavior is compared to analogous models analyzed with the developed analytically based calculation tool. The resulting strains are displayed in Fig. 5.

The principle decay behavior corresponds very well, small deviations can be observed for large length/width ratios (larger than 6:1).

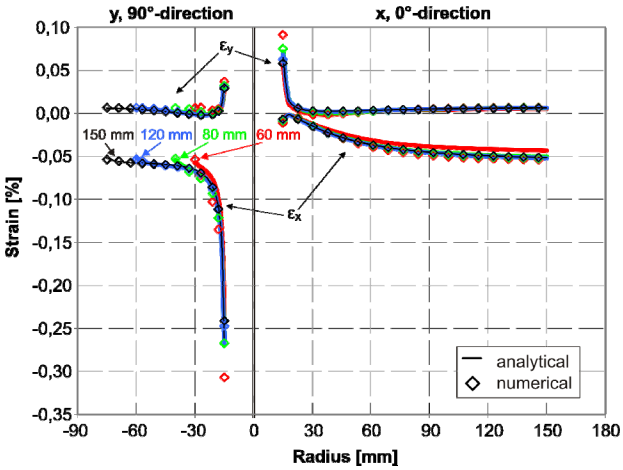


Fig. 5. Comparison of analytically calculated and numerically determined strains along the 0°- and 90°-radian at specimens with varying width and a constant free length of 700 mm

**Experimental determination of the strain decay behaviour**

For the realization of in-plane compression tests with thin-walled notched plate structures, the appropriate novel testing device is designed and built, based on the gained experiences of the finite element analysis [11]. The first prototype is set up using commercially available components. It features a modular setup with ball bearings between distance pieces on a solid axle at a molded frame. In first try outs, the simulated critical compressive force as well as the principle of the instability behavior were verified.

In a further development to the work of [10] the load application adapters are removed from the specimen. Instead adapters with guide slots are mounted to the compression platens of the testing machine. Therewith the specimens can be inserted easier and faster from the side. According to the previous simulations the distances of the supporting bearings were considered as upper limits.

Specimens of 80 mm to 150 mm width were examined with the present set-up of the novel testing de-

vice for in-plane compressive loads. The strain analysis is carried out at the central measuring field within the modular construction of the testing device. In load steps of 50 N the strains in x- and y-direction are determined (see example in Fig. 6).
In Fig. 7 the analytical and experimental results are compared. The principle behavior of the measured strains is consistent with those of the calculation. As expected and already experienced in former studies, the resolution of the steep strain gradients may be limited depending on the used size of the measuring area.

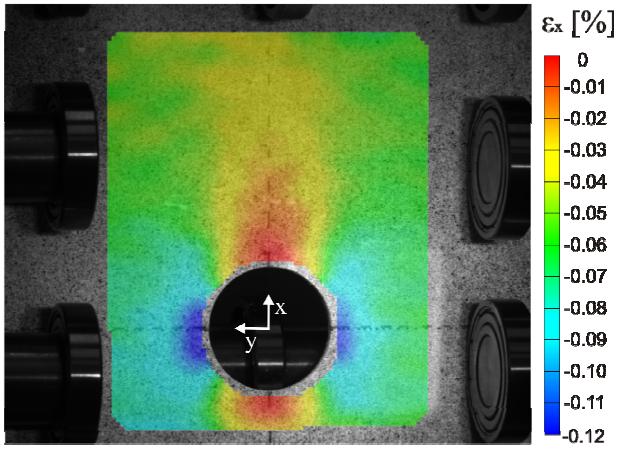


Fig. 6. Result of the measured decay behavior of the $\varepsilon_x$-strain of a 150 mm width specimen under an in-plane compressive force of $F_x$=3.75 kN

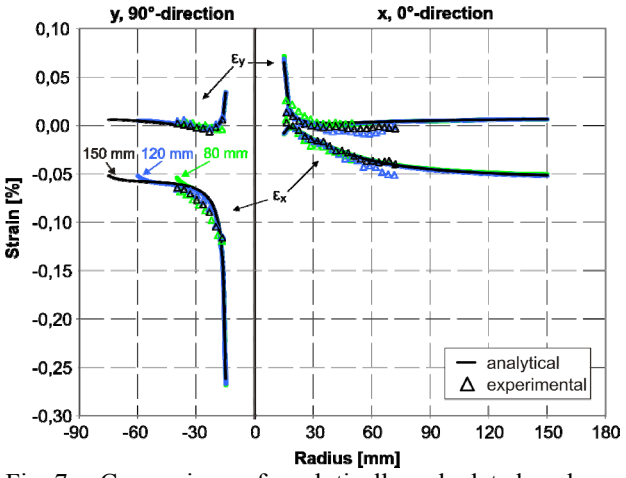


Fig. 7. Comparison of analytically calculated and experimentally measured strains along the 0°- and 90°-radian at specimens with varying width and a constant free length of 800 mm

### 3.3 Validation for bending load causing large deflections

Due to the presently investigated large size of the thin-walled composite plates with cut-out, only small strains at large deflections are reached under flexural loading.

**Numerical pilot survey and simulation of the strain decay behaviour**

The results of calculated and simulated flexural load cases at a chosen off-plane deformation of 120 mm are displayed in Fig. 8 for varying specimen width. In previously simulations and tests, this deformation was proven to induce strains well above the reachable strain measuring accuracy of the used optical measuring system. For the verification of the analytical model (based on the KIRCHHOFF-LOVE plate theory) the values of the transverse shear stiffness of the used shell elements (based on the MINDLIN-REISSNER plate theory) were raised in the FE-study (see also [5]). The difference to results gained without adjusted transverse shear stiffness is observable especially for the $\varepsilon_y$-strains on the 90°-radiant near the edge of the notch but it is only small.

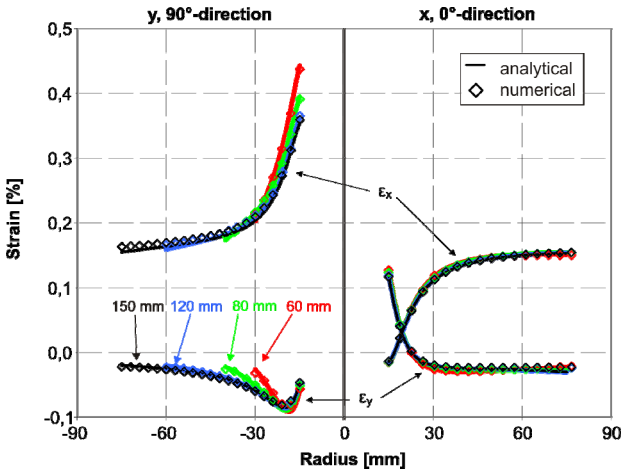


Fig. 8. Comparison of analytically calculated and numerically determined strains along the 0°- and 90°-radian at specimens with varying width and a constant length of 800 mm

**Evaluation and selection of a suited flexural testing device**

Conventional testing methods for the determination of flexural properties of materials and structures are not suited for the requirements of strain analysis of

notched thin-walled composite structures under large deflections. The three-point and four-point loading principles suggested in relevant nondestructive testing standards have been established for investigations on bending properties of fiber-reinforced polymer plate structures [see e.g. 12]. Due to the small thickness in relation to length and width, the specimens undergo large deflections already at small flexural strains. That is why common testing devices induce additional lateral and longitudinal forces in the specimen, also caused by the arrangement of the anvils of the flexure fixture working not frictionless. These combined load cases are not suited very well for the validation of the developed calculation methods because the in reality occurring boundary conditions are hard to define as input data for analytical and numerical calculation.

The in prior projects at the Institute of Lightweight Engineering and Polymer Technology (ILK) developed concept from [13] of a flexural testing device free of lateral and longitudinal force is better suited for the demands and is adaptable to the present specimen geometries. The flexural moment is induced to the specimen by rotation of the plate boundaries, induced by a hydraulic actuator and a special mechanism of the testing device. The compensation of the longitudinal force is realized by a moveable specimen bearing on one-side. In consequence, the region of the notch can move longitudinally as well as laterally while inducing the flexural moment (see also Fig. 9).

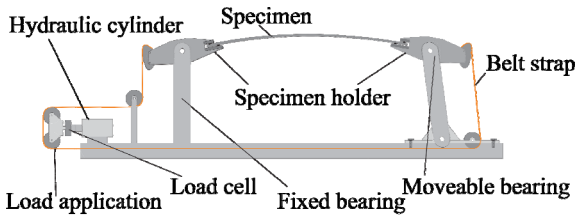


Fig. 9. Scheme of a flexural test device for large deflection free of lateral and longitudinal force [13]

**Setup of the optical measurement system**

Because of the large deflection of the measuring area, the user has to pay special attention that the measuring area stays in the viewing range of the cameras. Furthermore, the optical system for the investigation of the global displacement and distortional behavior has to be set-up in such a way, that the depth of the optical sharpness is larger than the flexural deformation in the off-plane direction, to ensure an undisturbed measurement process. In consequence, small details of the results as the steep strain gradients near the edge of the cut-out cannot be determined detailed.

The used test set-up is shown in Fig. 10.

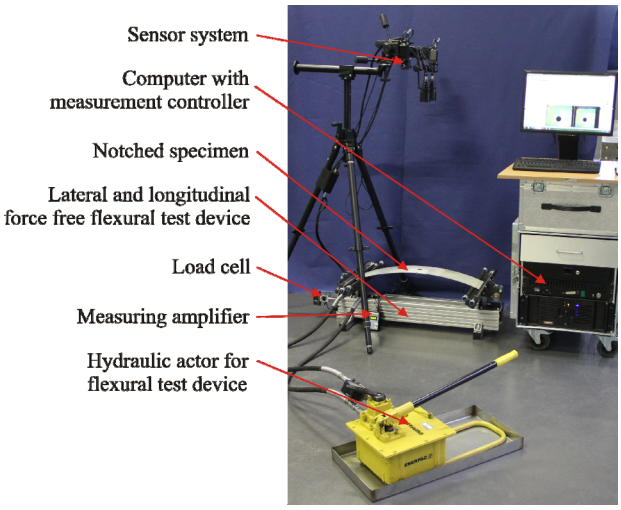


Fig. 10. Flexural test with test device free of lateral and longitudinal force with optical strain analysis with measurement system ARAMIS

The appliance of “smaller” measuring fields would allow the determination of more detailed results. However, it has to be considered that smaller measuring field sizes get an increased relative displacement on the result image. That is why the optical system often reaches the boundaries of its optical sharpness especially when laterally displacing the specimen. In Fig. 11 this context is shown exemplarily for a fixed positioned measuring system and a specimen moved in a flexure test.

For the experimental investigations, the specimens are loaded in such a way that the results are obtained in steps of 20 mm in the off-plane direction. The results presented here are determined at the maximum tested displacement of 120 mm in the off-plane direction. The comparison of the analytical and experimental results is displayed in Fig. 12 for chosen specimen widths of 60 mm and 150 mm at a measuring field size of 195x165 mm².

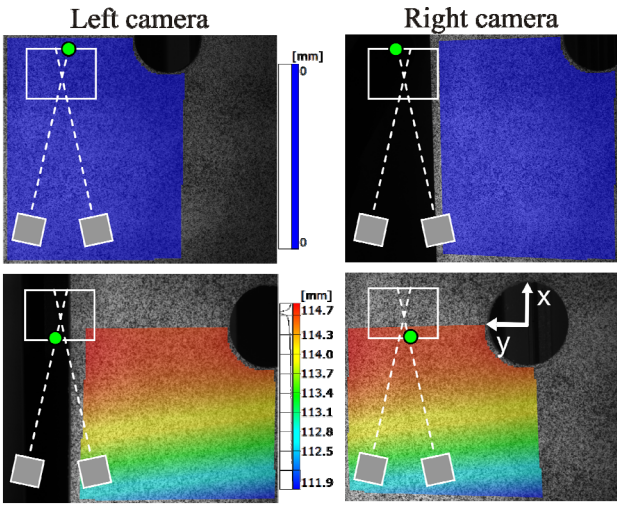


Fig. 11. Exemplary result for the displacement of the measurement region in flexure tests: undeformed reference (top), flexural deformation in the lateral and longitudinal direction of the region near the notch (bottom)

Here the results show a good correlation, but the known deficits from the used measurement technique near the edge of the notch are once again obvious.

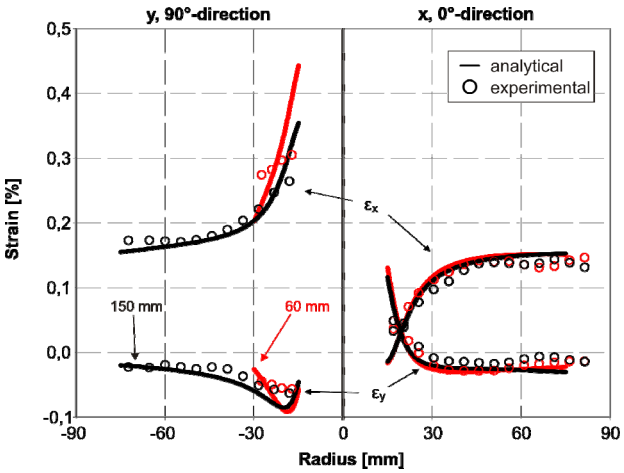


Fig. 12. Comparison of analytically calculated and experimentally measured strains along the 0°- and 90°-radian at specimens with varying width and a constant length of 800 mm (measuring field size: 195x165 mm²)

In the case of tensile or compression tests the measuring field size can be adapted very well for a better resolution of the strain gradients because of the only small field displacements. However, in flexure tests the depth of the optical sharpness of the measurement system as well as the longitudinal specimen displacement limits the use of small measurement fields at least in the case of a "fixed" measurement system.

**Increase of the resolution and use of a novel tracking method for relocated measuring fields for the experimental validation at flexure**

In the following a solution for the known displacement problems is presented based on the usage of a tracking system for the optical measurement system. Therefore a frame with two linear units with spindle drive for a two dimensional movement of the sensor system is placed above the flexural testing device.

The tracking system, the actuators and the sensors constitute a control loop. The change of the relative position of sensor and specimen is determined optically in real time with the same sensor as used by the measurement controller (capture frequency f=15 Hz). With the help of the software IVIEW (GOM mbH, Braunschweig, Germany), the position of a virtual measurement point is observed. The change of its coordinates is registered and passed to a special LABVIEW-based controller tool as a reference value. It axe-wise controls the position of the sensor till the prior relative position of sensor and measurement point is restored. To ensure the quality of the result images for the strain analysis, only those images are used that were captured when there is no movement of the sensor or the specimen. Further tests showed an excellent practicability of the developed tracking system for the strain analysis. The comparison of the investigations on different measuring field sizes showed that even the steep strain gradients near the notch can be observed. It also turned out that the choice of extremely small measuring areas also allows determining additional local strain effects. For the investigated PP/GF-knitted fabric material used in the SFB 639, these local results can even be correlated with the geometrical distribution of the single components within the used composite material. More information on the used tracking and measurement settings as well as their impact on the results is displayed in Tab. 4. In Fig. 13, a comparison of the experimental and analytical results is shown (analog to Fig. 12) for a smaller measuring field size of 50 x 40 mm².

Tab. 4. Influence of the dimensions of the measurement field size on the determined $\varepsilon_x$-results

| Measurement field | 195 x 165 mm² | 50 x 40 mm² |
|---|---|---|
| | 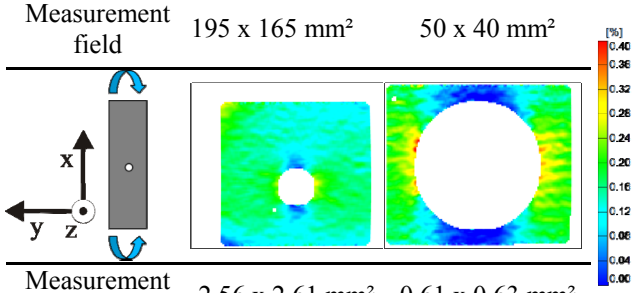 | |
| Measurement point size | 2.56 x 2.61 mm² | 0.61 x 0.63 mm² |
| Measurement point distance | $\Delta x$ = 1.71 mm<br>$\Delta y$ = 1.74 mm | $\Delta x$ = 0.41 mm<br>$\Delta y$ = 0.42 mm |
| Tracking speed | Not tracked | ~ 2 mm/s |

It can be observed, that the use of a tracking system for the optical measurement system allows the determination of steep strain gradients on structures undergoing large deformations. The correlation of the analytical and experimental results is very good considering the small impacts of the transverse shear effects on the $\varepsilon_y$-results, observed already in the numerical simulations at the 90°-radiant near the cut-out.

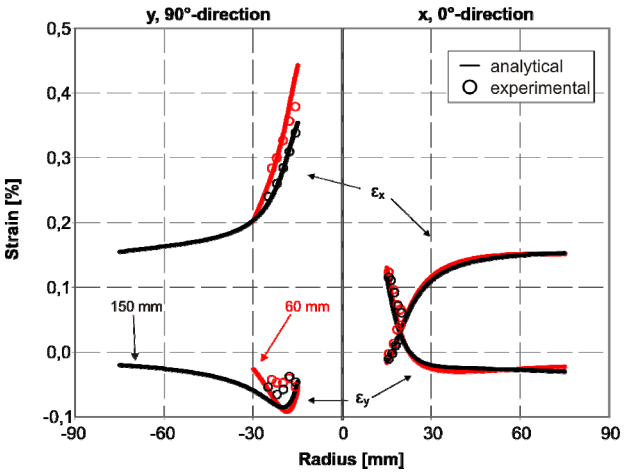


Fig. 13. Comparison of analytically calculated and experimentally measured strains along the 0°- and 90°-radian at specimens with varying width and a constant length of 800 mm (measuring field size: 50x40 mm²)

## 4 Discussion

The experimentally measured strain decay behaviours around the notch, which were used for validating the analytically based calculation tool, were obtained by an optical measuring technique which is well established in practical use. Fine differences of the experimental results to those of the analytical calculation have to be searched partially in the measurement accuracy of the used measurement system. A known solution to get increased resolutions of optically based results gained in experimental tests is the use of smaller measuring fields.
Occurring displacements of the object to be investigated can be compensated e.g. by tracking the measurement system. Here always the compromise between resolution and measurement field size has to be drawn. That is why actually the assembly of results gained from many small measurement field sizes with high resolution is under investigation.

In consequence of the good correlation of the analytical and experimental results, the ongoing numerical investigations are getting more complex by combining loading situations on plate structures and on more complex structures consisting of plane areas with cut-outs respectively. Parallel the analytically based calculation tool is used in the sense of a sub model in combination with numerical simulations. In that context it has to be clarified if and to what extent the regions with cut-out might also be slightly curved so that the analysis tool can also be used for a wider range of structures.

In the investigations, small deviation effects caused by large length/width ratio of the specimen are observed. This is mainly caused by the selection of the boundary collocation points on the boundary (see [2]). However since the presently used method is based on algorithms which work automatically, the dependency of the results on the length/width ratio (about 6:1) has to be considered. Nevertheless this length/width ratio covers a wide range which is large enough if using the analytically based calculation tool as sub model within numerical simulation systems. Here the user often will aspire to use nearly quadratic sub models where these shortcomings are avoided.

## 5 Conclusions

By using the developed analytically based calculation software in combination with standard FEM-software in the sense of an "analytical sub-model analysis" for the critical notched area, it offers the opportunity to take into consideration the effects of notches already during the first evaluations in the early state of the design process.
The newly developed measurement and testing technologies provide experimental conditions which are very close to the assumptions of calculation and simulation. This approach simplifies and assures the validation of the developed analytically based calculation method for notched fibre-reinforced multilayered composites.


## Acknowledgements

The authors would like to express their gratitude towards the Deutsche Forschungsgemeinschaft (DFG), who funds the subproject B2 within the scope of the Collaborative Research Centre SFB 639 "Textile-Reinforced Composite Components in Function-Integrating Multi-Material Design for Complex Lightweight Applications".


## References


[1] W. Hufenbach, B. Grüber, R. Gottwald, M. Lepper and B. Zhou „Analytical and experimental analysis of stress concentrations in notched multilayered composites with finite outer boundaries." *Mech Compos Mater*, 46(5), pp. 531-538, 2010. doi: 10.1007/s00419-012-0641-5.

[2] W. Hufenbach, B. Grüber, M. Lepper, R. Gottwald and B. Zhou „An analytical method for the determination of stress and strain concentrations in textile-reinforced GF/PP-composites with elliptical cutout and a finite outer boundary and its numerical verification." *Arch Appl Mech*, Vol. 83, Issue 1, pp 125-135, 2013. doi: 10.1007/s00419-012-0641-5.

[3] S. G. Lekhnitskii "Anisotropic Plates" Transl. 2nd russ. print run: S. W. Tsai and T. Cheron, Gordon and Breach, New York et al. 1968.

[4] W. Becker "Complex method for the elliptical hole in an unsymmetric laminate", *Archiv of Applied Mechanics*, 63, pp 159-169, 2000.

[5] B. Grüber „Beitrag zur Strukturanalyse von anisotropen Schichtverbunden mit elastischen Einschlüssen und Bolzen", Diss. TU Dresden, 2004.

[6] N.N., ASTM D 6484/D 6484M – 04, "Standard Test Method for Open-Hole Compressive Strength of Polymer Matrix Composite Laminates", 2004.

[7] www.gom.com, April 2013.

[8] N.N., DIN EN ISO 14126, „Faserverstärkte Kunststoffe - Bestimmung der Druckeigenschaften in der Laminatebene", December 2000.

[9] N.N., „Vorrichtung zur mechanischen Werkstoffprüfung", Gebrauchsmuster DE20314761U1, Dresden, 2003.

[10] W. Hufenbach, B. Grüber, R. Gottwald, M. Lepper and B. Zhou „Novel testing device for the experimental stress concentration analysis of multilayer textile composites under in-plane compressive load." *14th Symposium on Experimental Stress Analysis and Materials Testing*, submitted for publication in ISI Proceedings. April 2013.

[11] Hufenbach et al. „Vorrichtung zur einachsigen Druckprüfung schlanker Prüfkörper" patent application DE 10 2010 052 815, 2012.

[12] N.N., DIN EN ISO 14125, „Faserverstärkte Kunststoffe – Bestimmung der Biegeeigenschaften", Mai 2011.

[13] J. Jaschinski „Zum Strukturverhalten dünnwandiger Leichtbau-Sandwichbleche", Diss. TU Dresden 2012.